Influence of the Clay Modification and Compatibilizer on the Structure and Mechanical Properties of Ethylene–Propylene–Diene Rubber/Montmorillonite Composites

Hua Zheng, Yong Zhang, Zonglin Peng, Yinxi Zhang

State Key Laboratory of Metal Matrix Composites, School of Chemistry and Chemical Technology, Shanghai Jiao Tong University, Shanghai 200240, China

Received 22 April 2003; accepted 1 August 2003

ABSTRACT: Ethylene–propylene–diene rubber (EPDM)/montmorillonite (MMT) composites were prepared through a melt process, and three kinds of surfactants with different ammonium cations were used to modify MMT and affect the morphology of the composites. The morphology of the composites depended on the alkyl ammonium salt length, that is, the hydrophobicity of the organic surfactants. Organophilic montmorillonite (OMMT), modified by octadecyltrimethyl ammonium salt and distearyldimethyl ammonium salt, was intercalated and partially exfoliated in the EPDM matrix, whereas OMMT modified by hexadecyltrimethyl ammonium chloride exhibited a morphology in which OMMT existed as a common filler. Ethylene–propylene–diene rubber grafted with maleic anhydride (MAH-*g*-EPDM) was used as a compatibilizer and greatly affected the dispersion of OMMT. When OMMTs were modified by octadecyltrimethyl ammonium chloride and distearydimethyl ammonium chloride, the EPDM/OMMT/MAH-*g*-EPDM composites (100/15/5) had an exfoliated structure, and they showed good mechanical properties and high dynamic moduli. © 2004 Wiley Periodicals, Inc. J Appl Polym Sci 92: 638–646, 2004

Key words: clay; composites; mechanical properties; morphology

INTRODUCTION

Polymer–clay nanocomposites have been extensively studied in recent years because they often exhibit physicochemical properties dramatically different from those of their microcomposite and macrocomposite counterparts.[1] Two major findings have been important for the revival of these materials. First, nylon-6/montmorillonite (MMT) composites have been reported to have remarkably enhanced thermal and mechanical properties.[2,3] Second, polymers and clay have been melt-mixed without the use of organic solvents.[4]

For the efficient improvement of the properties of polymer–MMT composites, the basal spacing of MMT should be made accessible to the polymer chains; this may be realized through cation exchange between MMT and organic ammonium salts, which yields organophilic montmorillonite (OMMT). In contrast to silica fillers, in which matrix–filler and filler–filler interactions can be controlled by surface modification with silanes, the cation exchange in silicates changes the aggregate structure by increasing the interclay distance through the intercalation of organophilic alkyl cations into interlayers.[5] Depending on the degree of polymer penetration into the silicate framework, the polymer–MMT nanocomposites can be classified as intercalated or exfoliated nanocomposites.[6,7] In intercalated nanocomposites, clay particles are dispersed in an ordered lamellar structure with a larger gallery height via the insertion of polymer chains into the gallery. In exfoliated nanocomposites, each silicate layer of clay particles is delaminated and dispersed in a continuous polymer matrix.

Rubber–clay nanocomposites have drawn much attention in recent years.[8–13] Okada et al.[14] reported that acrylonitrile–butadiene rubber (NBR) filled with 10 phr organoclay had a tensile strength comparable to that of NBR filled with 40 phr carbon black. Another major effect was the reduced gas permeability of styrene–butadiene rubber/clay composites, which suggested their application as tire innerliners.[15] Because ethylene–propylene–diene rubber (EPDM) is a widely used rubber, EPDM–clay composites should have great commercial potential. However, EPDM does not include any polar groups in its backbone; therefore, the homogeneous dispersion of clay layers in an EPDM matrix would be difficult to realize. Recently, Chang et al.[16] reported the intercalated structure of an EPDM/OMMT nanocomposite containing octade-

Correspondence to: Y. Zhang (yong_zhang @sjtu.edu.cn).

Journal of Applied Polymer Science, Vol. 92, 638–646 (2004)

cylammonium ions ($C_{18}H_{37}NH_3^+$) and liquid EPDM, in which the presence of fairly large stacks of clay layers indicated a poor dispersion of clay. Usuki et al.[17] reported that EPDM/OMMT composites showed an exfoliated morphology when the melt-blending temperature was 200°C.

Layered silicates existing on a nanoscale are effective reinforcements for rubber materials.[5,10–15] However, the complete and homogeneous dispersion of individual silicate layers in a rubber matrix is difficult to realize, and there are still no generally applicable guidelines for the optimum rubber/layered-silicate combination, especially by means of a conventional rubber-compounding process. In this study, EPDM/OMMT composites were prepared through melt blending at 90°C. Three kinds of surfactants with different ammonium ions were used to modify MMT. The morphology of the composites was investigated. Ethylene–propylene–diene rubber grafted with maleic anhydride (MAH-*g*-EPDM) was used as a compatibilizer to promote the dispersion of OMMT in EPDM.

EXPERIMENTAL

Materials

EPDM (4770R; ethyldiene norborene (ENB) type) was supplied by DuPont Co. (United States) with an ethylene content of 70% and an ML_{1+4} value of 70 at 100°C. Na-type montmorillonite (Na-MMT) was made by Zhejiang Fenghong Clay Chemicals Co. (Zhejiung, China) with a charge-exchange capacity (CEC) of 110 mequiv/100 g. Hexadecyltrimethyl ammonium chloride, octadecyltrimethyl ammonium chloride, and distearydimethyl ammonium chloride were produced by Akzo Nobel Chemicals Co. (Holland). Other ingredients, such as sulfur, zinc oxide, stearic acid, and *N*-cyclohexyl-2-benzothiazile sulfenamide (CZ), were obtained from Shanghai Jiacheng Chemicals Co. (Shanghai, China) and were used without further purification. MAH-*g*-EPDM was made in our laboratory with 2,5-dimethyl-2,5-bis(*tert*-butyl peroxy) hexane as an initiator in a Haake (Germany) Rheocord RC90 twin-screw extruder at 220°C.

Preparation of OMMT

MMT was modified with various alkyl ammonium salts according to reported methods.[18] Na-MMT (100 g) was dispersed in 5000 mL of hot water at 80°C under continuous stirring to obtain a suspension solution. Hexadecyltrimethyl ammonium salt (32.7 g, 115 mmol) and 11.5 mL of concentrated hydrochloric acid were dissolved in 2000 mL of hot water at 80°C, and the resultant solution was poured into the hot MMT–water suspension solution under vigorous stirring for about 5 min to yield a white precipitate. The precipitate was collected on a cloth filter, washed three times with 2500 mL of water at 80°C, and then freeze-dried to yield a hexadecyltrimethy ammonium salt modified MMT (MMT-C16). The modification of MMT with octadecyltrimethyl ammonium salt or distearyldimethyl ammonium salt followed the aforementioned procedure, except that 35.9 g of octadecyltrimethyl ammonium salt (115 mmol) or 63.3 g of distearyldimethyl ammonium salt (115 mmol) was used instead of 32.7 g of hexadecyltrimethyl ammonium salt, and the resultant OMMTs were denoted MMT-C18a and MMT-C18b, respectively. The structural information and X-ray diffraction (XRD) patterns of these OMMTs are shown in Figure 1.

Preparation of the EPDM/OMMT composites

EPDM, OMMT (15 phr), and MAH-*g*-EPDM (5 phr) were melt-mixed in a Haake RC90 rheometer for 5 min at 90°C and a rotor speed of 136 rpm, and this was followed by the addition of 5 phr zinc oxide, 1 phr stearic acid, 1.8 phr sulfur, and 1.5 phr CZ; the mixing lasted another 5 min. The resultant mixture was pressed into sheets on a two-roll mill at the ambient temperature and was compression-molded at 175°C for the optimum cure time to yield a rubber vulcanizate.

Characterization

XRD was carried out with a diffractometer (D/max-IIIA, Japan) with Cu Kα radiation at a generator voltage of 40 kV and a generator current of 100 mA. The diffractogram was scanned in a 2θ range of 1–10° at a rate of 4°/min. Transmission electron microscopy (TEM) observations were performed of ultrathin sections of the films with a JEM-100CX-III (JEOL Co., Japan) at an acceleration voltage of 120 kV. A thermogravimetric analysis (TGA) was conducted with a thermal analyzer (TGA 7e, PerkinElmer, United States) under an N_2 flow at a heating rate of 20°C/min. Tensile tests were carried out with an Instron (New York) 4465 tester at a deformation of 500 mm/min according to ASTM D 412. The dynamic mechanical properties were determined with a dynamic mechanical test analyzer (PE-DMTA7e, PerkinElmer). The experimental samples were subjected to a cyclic tensile strain with an amplitude of 0.15% at a frequency of 10 Hz and a scanning rate of 2°C/min at $-90 \sim 20$°C.

MAH-*g*-EPDM samples were dried in a vacuum oven at 80°C for 8 h and were then dissolved in xylene and precipitated with acetone. The precipitants were dried in a vacuum oven at 80°C for 24 h. The maleic anhydride (MAH) content was determined by elemental analysis (CE EA-1110, United States). All the data for the MAH contents are summarized in Table I.

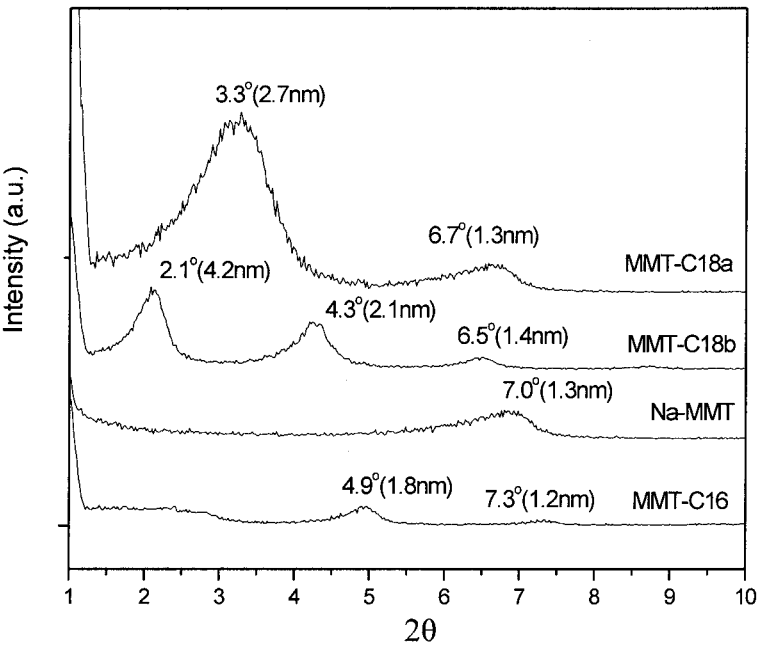

Figure 1 XRD patterns of Na-MMT and OMMTs.

RESULTS AND DISCUSSION

The TGA curves of Na-MMT and OMMTs are shown in Figure 2. The first stage of decomposition is in the temperature range of 45–100°C. Na-MMT is associated with a relatively higher weight loss (ca. 7.9%), corresponding to the removal of water from the interlayers coordinated to Na^+. For the three OMMTs, the weight loss in the temperature range is about 5.8% because of the organophilic properties of OMMTs containing alkyl ammonium ions. Shulai et al.[19] observed similar behavior in pyridine-treated sepiolite and palygorskite.

The weight loss in the temperature range of 100–600°C for Na-MMT is about 2.6% and can be attributed to the decomposition of hydrogen-bonded water molecules and some of the OH groups from tetrahedral sheets.[20] The weight losses of the OMMTs are greater: 19% for MMT-C16, 27.4% for MMT-C18a, and 42.4% for MMT-C18b. The weight losses for the OMMTs may be explained mainly by the decomposition of intercalated ammonium and partly by the adsorbed water molecules below 220°C.[21]

TABLE I
MAH Content in MAH-*g*-EPDM Prepared by Reactive Extrusion

EPDM (wt %)	MAH (wt %)	MAH content in MAH-*g*-EPDM (wt %)
98	2	0.9
96	4	1.9
94	6	3.8
90	10	5.2
88	12	8.5

The weight losses in the temperature range of 600–800°C for all OMMTs and Na-MMT are approximately 8.0% and are associated with the dehydroxylation of Na-MMT.[22,23]

As shown in Figure 3, the diffraction peaks of the EPDM/Na-MMT and EPDM/MMT-C16 composites are unchanged in comparison with those of Na-MMT and MMT-C16, and the diffraction peaks are still at $2\theta = 7°$ and $2\theta = 4.9°$, respectively. This indicates that there are few EPDM chains intercalated into the interlayers of Na-MMT and MMT-C16. The EPDM composites containing Na-MMT and MMT-C16 have the same structure as conventional composites.[24] On the contrary, the EPDM composites containing MMT-C18a and MMT-C18b have broader peaks in their XRD patterns than MMT-C18a and MMT-C18b. The basal spacings of the EPDM/MMT-18a and EPDM/MMT-18b composites are 4.08 and 5.44 nm, respectively, having increased by 1.41 and 1.28 nm with respect to those of MMT-18a and MMT-18b. The changes in the basal spacings indicate that intercalation of EPDM chains into OMMT occurs, with some OMMT layers possibly being exfoliated and dispersed in the EPDM matrix.

For the preparation of EPDM–clay nanocomposites, the modification of Na-MMT is essential, and the chain length of the organic surfactant, that is, the hydropho-

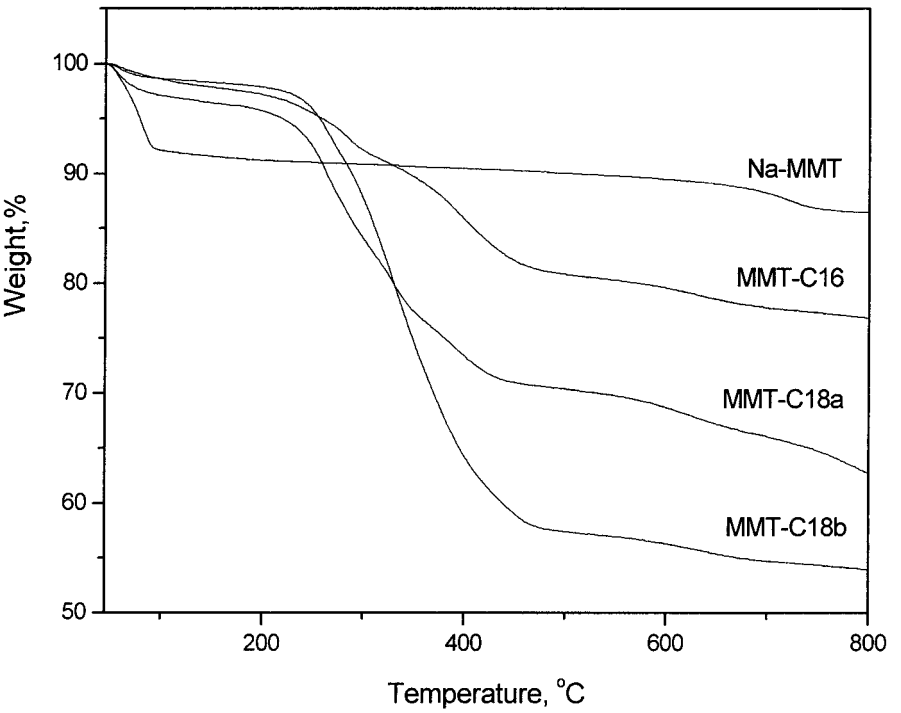

Figure 2 TGA curves of Na-MMT and OMMTs.

bicity, is important.[24] An intercalated structure can be obtained when the number of methylene groups in alkyl ammonium is greater than 16, and the results agree with the nanocomposite formation of a maleic anhydride grafted polyethylene (PEMA)/clay system.[24]

Figure 4 shows a TEM micrograph of an EPDM/MMT-C18b composite (100/15). The dark zones are the cross sections of the MMT-C18b layers. The MMT-C18b particles, 300–500 nm thick, are uniformly dispersed in the EPDM matrix. This indicates that the silicate layers are not fully exfoliated but instead are stacked, with several layers in the form of an intercalated layer structure in the EPDM matrix.

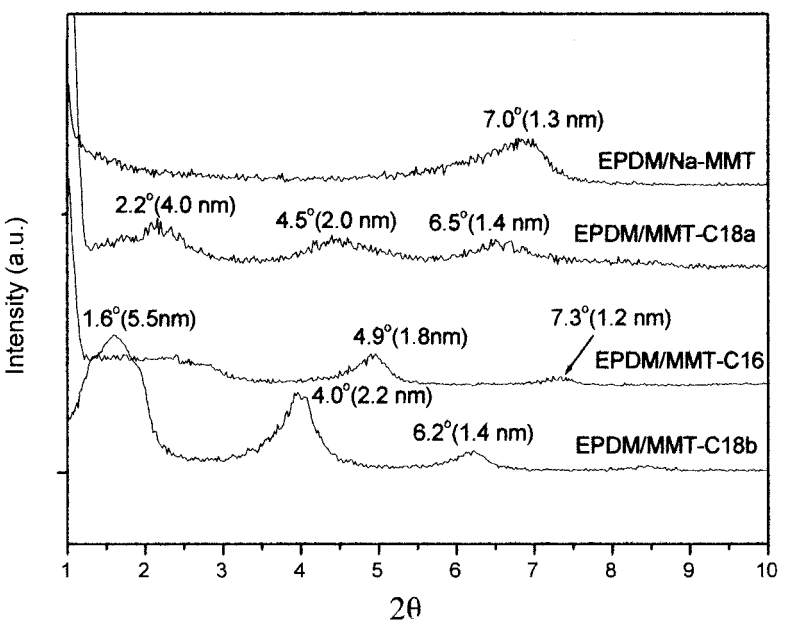

Figure 3 XRD patterns of EPDM/MMT (OMMT) composites.

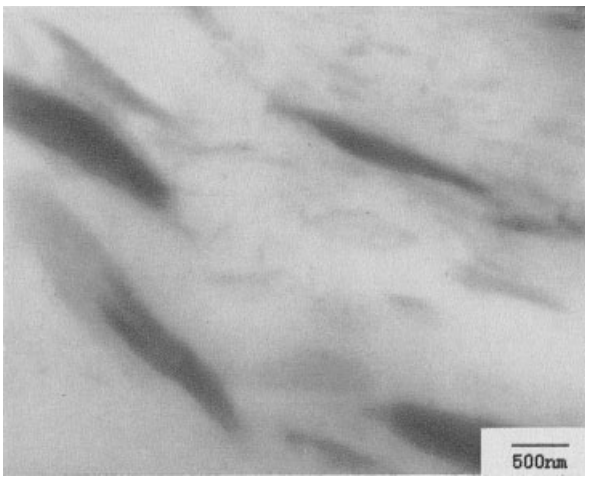

Figure 4 TEM micrograph of an EPDM/MMT-C18b composite (100/15).

Effect of MAH-*g*-EPDM on the morphology of the EPDM–clay composites

MAH-grafted polymers have been used as compatibilizers for some hydrophobic polymer–MMT nanocomposites.[25–27] The XRD patterns of EPDM/MAH-*g*-EPDM/OMMT composites are shown in Figures 5–7. The presence of MAH-*g*-EPDM leads to a remarkable change in the phase structure of the composites. The diffraction peaks of the EPDM/MMT-C18a composites disappear completely when the MAH content is about 5.2%. The interaction between OMMT and MAH-*g*-EPDM affects the dispersion of OMMT. When EPDM, MAH-*g*-EPDM, and OMMT are mixed together, MAH-*g*-EPDM should easily penetrate the interlayers of OMMT. This depends on the strong hydrogen-bonding interaction and a condensation reaction between anhydride groups in MAH and amine groups in OMMT and leads to the expansion of interlayer spacings and a further weakening of the interactions between the silicate layers.[28] This facilitates the intercalation of EPDM chains into the silicate galleries and results in the formation of the exfoliated structure.

At present, it is more difficult to explain why there is no diffraction peak for EPDM/MMT-C18b composites containing MAH-*g*-EPDM as a compatibilizer, even though the MAH content is very low. A possible reason may be that the surfactant in MMT-C18b has a longer molecular chain and a higher interlayer spacing (4.2 nm) than that in MMT-18a (2.7 nm).

The EPDM/MAH-*g*-EPDM/MMT-C16 composites show clear peaks at the same position at which MMT-C16 does, and this indicates the absence of the intercalation of EPDM chains into MMT-C16, even though MAH-*g*-EPDM with a higher MAH content has been used.

TEM micrographs have been used to confirm the dispersion of OMMT (Fig. 8). Significant stacks of MMT-C18a and MMT-C18b have not been found in the two composites, and the silicate layers are exfoliated and dispersed uniformly as monolayers and a

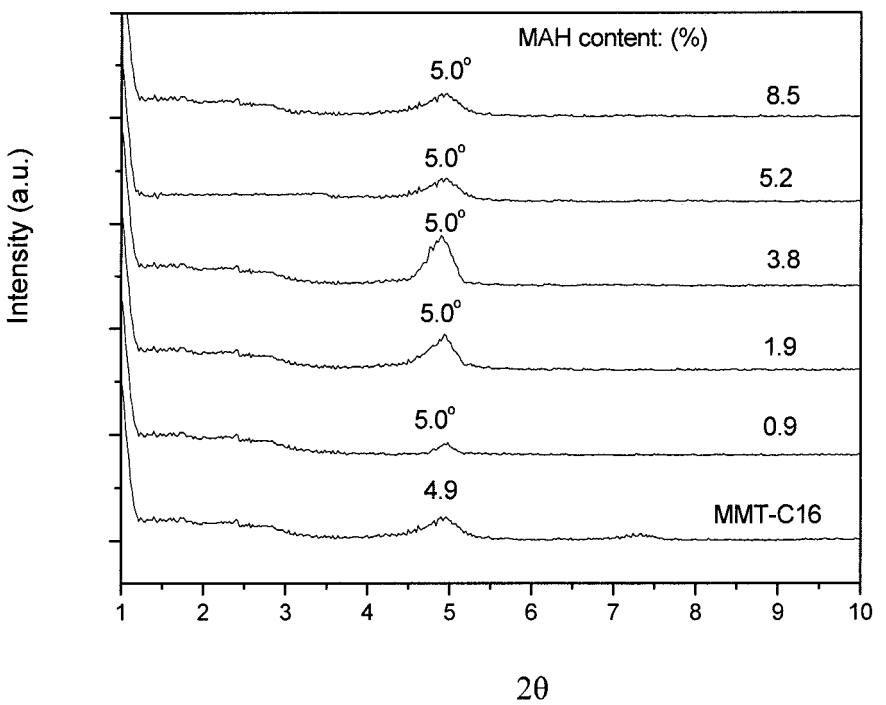

Figure 5 XRD patterns of EPDM/MMT-C16/MAH-*g*-EPDM composites (100/15/5).

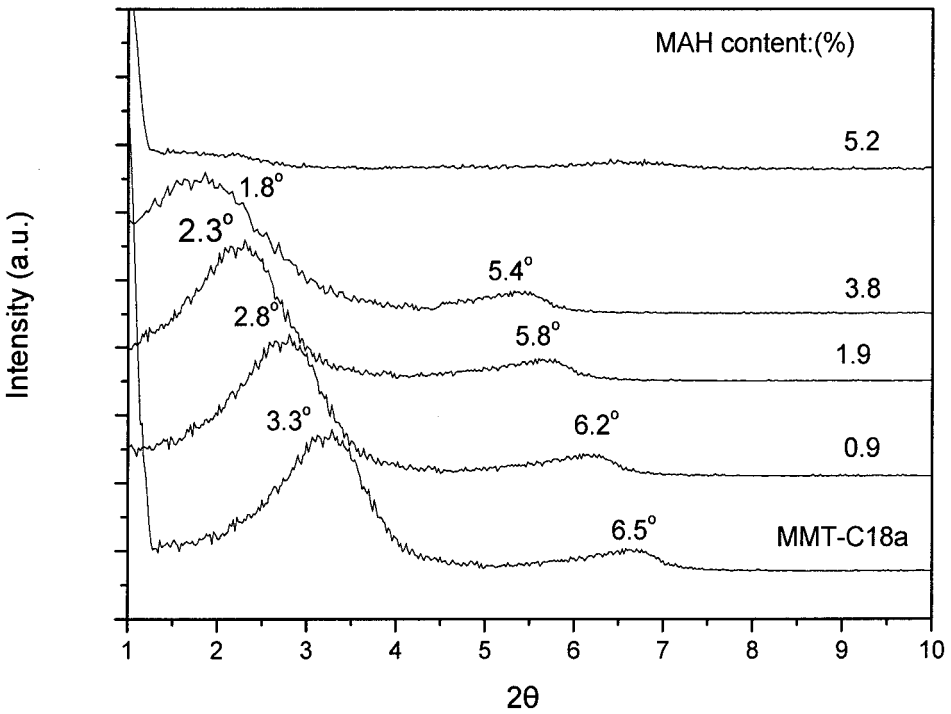

Figure 6 XRD patterns of EPDM/MMT-C18a/MAH-*g*-EPDM composites (100/15/5).

few layers; this indicates that MAH-*g*-EPDM acts as an efficient compatibilizer for the dispersion of OMMTs in the systems. In other words, the insufficient breakup force of the EPDM matrix is compensated by the reduction of interfacial tension between EPDM and MMT-C18a and MMT-C18b, and this facilitates the dispersion process [Fig. 8(b,c)].[24] There are agglomerates existed in the EPDM/MMT-C16/MAH-*g*-EPDM composites, as confirmed by the XRD patterns, indicating that the hydrophobicity of organically modified Na-MMT is crucial to the nanocomposite formation shown in Figure 8.[24]

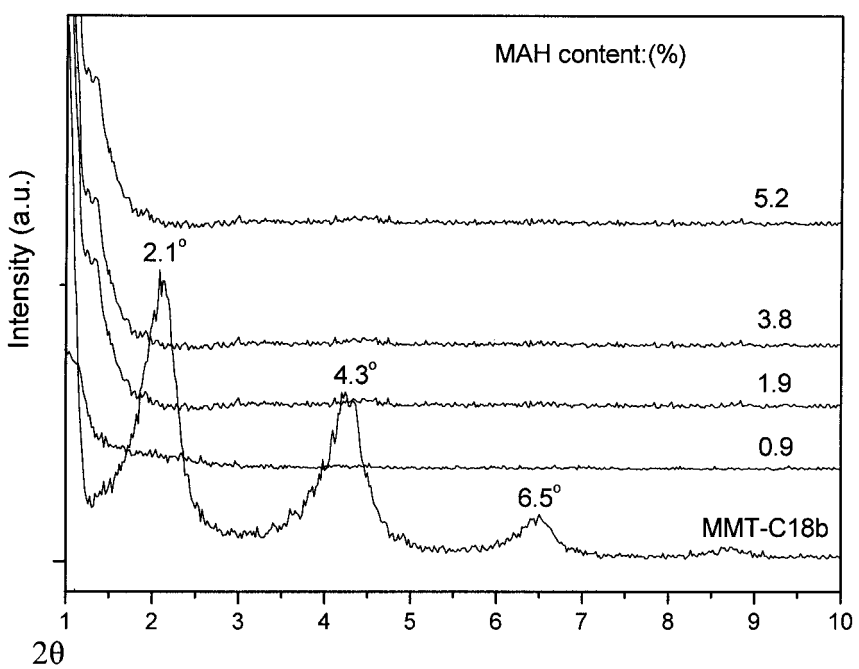

Figure 7 XRD patterns of EPDM/MMT-C18b/MAH-*g*-EPDM composites (100/15/5).

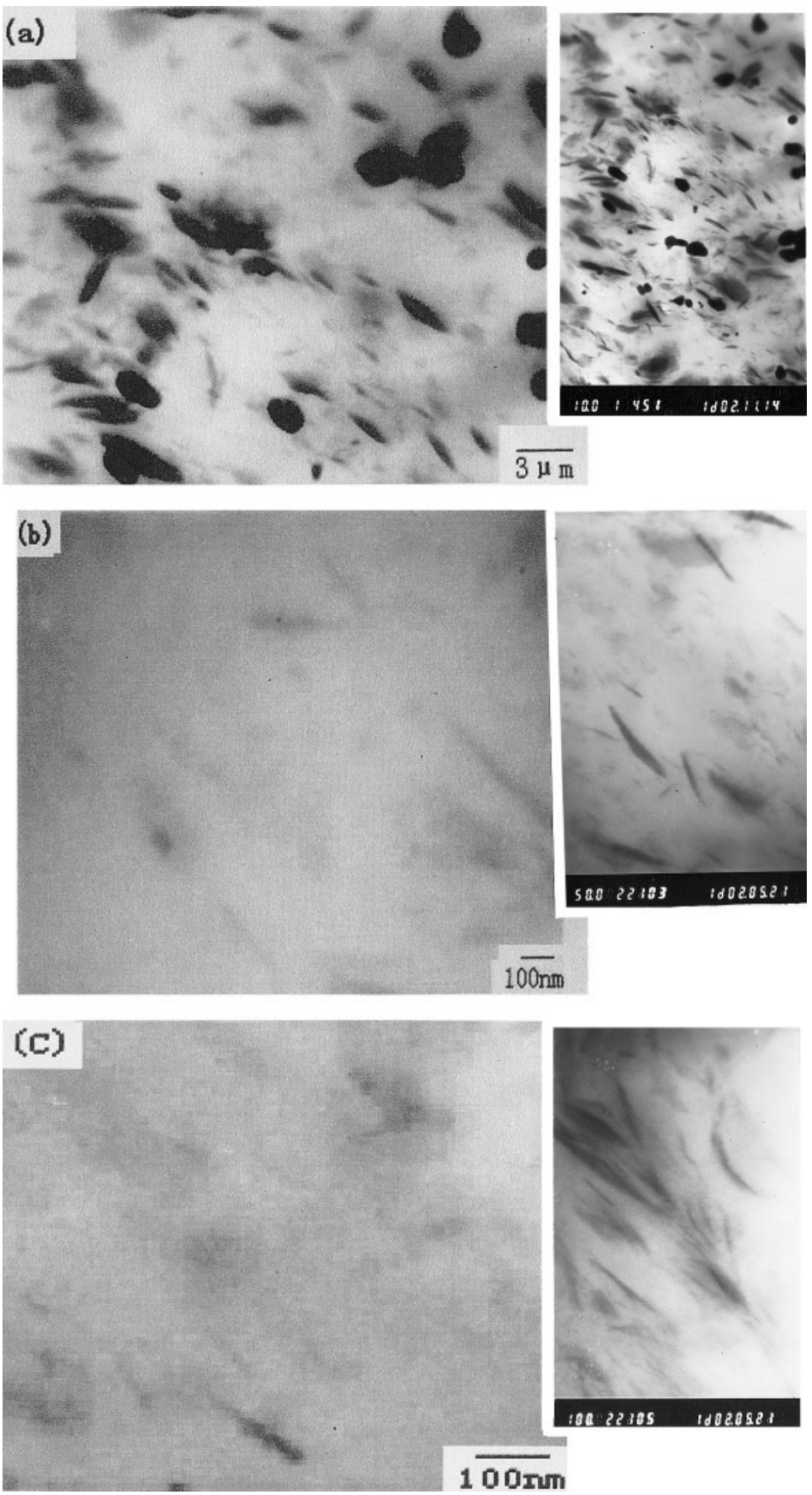

Figure 8 TEM micrographs of EPDM/OMMT/MAH-*g*-EPDM composites (100/15/5, 5.2% MAH content): (a) EPDM/MMT-C16/MAH-*g*-EPDM, (b) EPDM/MMT-C18a/MAH-*g*-EPDM, and (c) EPDM/MMT-C18b/MAH-*g*-EPDM.

TABLE II
Mechanical Properties of EPDM/OMMT Composites

Propertys	Gum EPDM vulcanizate	EPDM/MMT-C18a	EPDM/MMT-C18b	EPDM/MMT-C18a/MAH-*g*-EPDM	EPDM/MMT-C18b/MAH-*g*-EPDM
Tensile strength (MPa)	4.8	13.8	15.5	21.9	22.2
Elongation at break (%)	275	420	470	550	620
Modulus at 100% extension (MPa)	1.90	2.5	2.8	3.8	3.6
Modulus at 300% extension (MPa)	—	3.8	5.2	5.6	5.2
Tear stress (kN m^{-1})	25.4	38.4	42.6	52.1	54.6
Hardness (Shore A)	67	72	71	72	73

EPDM/OMMT/MAH-*g*-EPDM: 100/15/5; MAH content = 5.2%.

Mechanical properties of the EPDM/OMMT composites

The intercalation of rubber chains provides the EPDM/OMMT composites with outstanding mechanical properties (Table II). The tensile strength of the composites is 3–4 times higher than that of an EPDM gum vulcanizate. The moduli at 100 and 300% of the composites are higher than those of EPDM. The EPDM/MAH-*g*-EPDM/MMT-C18b composite has the highest tensile strength (22.2 MPa) and elongation at break (620%).

The effects of MAH-*g*-EPDM on the dynamic moduli of EPDM composites containing MMT-C18a and MMT-C18b are shown in Figure 9. The dynamic storage moduli of the composites containing MAH-*g*-EPDM are higher than those of the composites without MAH-*g*-EPDM, and this indicates that strong interfacial action exists in the composites containing MAH-*g*-EPDM.

CONCLUSIONS

EPDM/MMT composites with intercalated and exfoliated structures have been prepared through a polymer melt-intercalation process. The morphology of the composites depends on the alkylamine chain length, that is, the hydrophobicity of the organic surfactants. OMMTs modified by octadecyltrimethyl ammonium chloride and distearydimethyl ammonium chloride can be intercalated and partially exfoliated in an EPDM matrix. An EPDM composite filled with hexadecyltrimethyl ammonium chloride modified OMMT exhibits the morphology of a conventional composite because of the lower hydrophobicity.

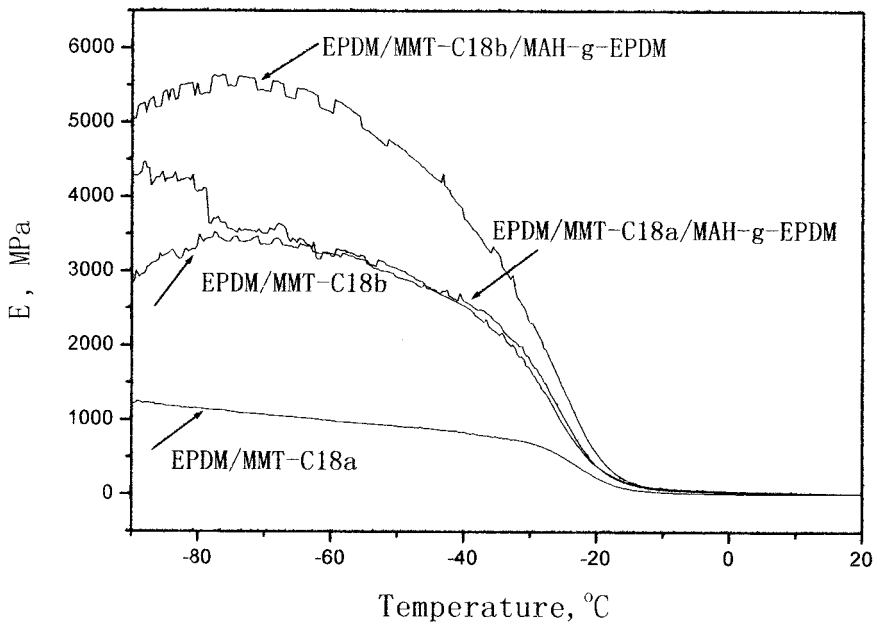

Figure 9 Effect of MAH-*g*-EPDM on the dynamic moduli of EPDM/OMMT composites (100/15/5, 5.2% MAH content).

MAH-*g*-EPDM has a significant influence on the dispersion of OMMT in EPDM composites, which depends on the MAH content in MAH-*g*-EPDM. When the MAH content is 5.2% and the OMMTs are modified by octadecyltrimethylamine and distearyldimethylamine, EPDM/OMMT/MAH-*g*-EPDM composites (100/15/5) have exfoliated structures and show great improvements in the mechanical properties and dynamic properties.

References

1. Alexandre, M.; Dubois, P. Mater Sci Eng 2000, 28, 1.
2. Usuki, A.; Kawasumi, T.; Kojimi, M.; Fukushima, Y.; Okada, A.; Kurauche, T.; Kamiganto, O. Mater Res 1993, 8, 1179.
3. Kojima, Y.; Usuki, A.; Kawasumi, M.; Okade, A.; Kurauchi, T. T.; Kamigaito, O. J Polym Sci Part A: Polym Chem 1993, 31, 983.
4. Vaia, R. A.; Ishiii, H.; Giannelis, E. P. Chem Mater 1993, 5, 1694.
5. Ganter, M.; Gronski, W.; Semke, H.; Zilg, C.; Thomann, C. Kautsch Gummi Kunstst 2001, 4, 166.
6. Lebaron, P. C.; Wang, Z.; Pinnavaia, T. J. Appl Clay Sci 1999, 15, 11.
7. Zanetti, M.; Lomakin, S.; Camino, G. Macromol Mater Eng 2000, 279, 1.
8. Burnside, S. D.; Giannelis, E. P. J Polym Sci Part B: Polym Phys 2000, 38, 1595.
9. Zhang, L. Q.; Wang, Y. Z.; Wang, Y.; Sui, Y.; Yu, D. J Appl Polym Sci 2000, 78, 1873.
10. Wang, Y.-Z.; Zhang, L.-Q.; Tang, C.-H.; Yu, D. S. J Appl Polym Sci 2000, 78, 1879.
11. Kojima, Y.; Fukumori, K.; Usuki, A.; Okada, A.; Kurauchi, T. Mater Sci Lett 1993, 12, 889.
12. Mousa, A.; Karger, K. J Macromol Mater Eng 2001, 286, 260.
13. Markus, G.; Wolfram, G.; Peter, R.; Rolf, M. Rubber Chem Technol 2001, 74, 221.
14. Okada, A.; Usuki, A.; Kurauchi, T.; Kamigaito, O. In Hybrid Organic–Inorganic Composites; Mark, J. E.; Lee, C. Y. C.; Bianconi, P. A., Eds.; ACS Symposium Series 585; American Chemical Society: Washington, DC, 1995, pp 55–65.
15. Wang, Y. Z.; Zhang, L. Q.; Tang, C. H. J Appl Polym Sci 2000, 78, 1879.
16. Young, W. C.; Yungchu, Y.; Seunghoon, R.; Changwoon, N. Polym Int 2002, 51, 319.
17. Usuki, A.; Tukigase, A.; Kato, M. Polymer 2002, 43, 2185.
18. Masaya, K.; Hasegawa, N.; Kato, M.; Usuki, A.; Okada, A. Macromolecules 1997, 30, 6333.
19. Shuali, U.; Yariv, S.; Steihberg, M.; Muller, V. M.; Kahr, G. A Rubber Clay Miner 1991, 26, 497.
20. Bray, H. J.; Redfern, S. A. T.; Clark, S. M. Miner Mag 1998, 62, 647.
21. Bala, P.; Samantaray, B. K.; Srivastava, S. K. Mater Res Bull 2000, 35, 1717.
22. Brindley, G. W. Int Miner Ass Pap Proc Gen Meet 1971, 1, 70.
23. Olphen, H. V.; Fripiat, J. J. Data Handbook for Clay Materials and Other Non-Metallic Minerals; Pergamon: Oxford, 1979.
24. Wang, K. H.; Choi, M. H.; Koo, C. M.; Choi, Y. S. Polymer 2001, 42, 9819.
25. Ide, F.; Hasegawa, A. J Appl Polym Sci 1974, 18, 963.
26. Dagli, S. S.; Xanthos, M.; Biesenberger, J. A. Soc Plast Eng Annu Tech Conf Tech Paper 1990, 36, 1924.
27. Gonzales, M. A.; Keskkula, H.; Paul, D. R. J Polym Sci Part B: Polym Phys 1995, 33, 1751.
28. Kyu, N. K.; Hyungsu, K.; Jae, W. L. Polym Eng Sci 2001, 41, 1963.